NRC Research Press

ARTICLE

A poststratified ratio estimator for model-assisted biomass estimation in sample-based airborne laser scanning surveys

Anna H. Ringvall, Göran Ståhl, Liviu T. Ene, Erik Næsset, Terje Gobakken, and Timothy G. Gregoire

Abstract: To estimate the aboveground biomass (AGB) for large areas, two-stage sampling designs using airborne laser scanning (ALS) as a strip sampling tool in combination with subsampling of field plots have been successfully applied in several studies. However, the studies have pointed to problems in the proposed estimator, partly related to the unequal length of flight lines in irregularly shaped areas. In this article, we present a model-assisted ratio estimator for such two-stage designs utilizing the area of the ALS strip as the auxiliary variable. The proposed estimator is further developed for estimation in subpopulations and for poststratified estimation. When deriving a variance estimator of the poststratified estimator, we considered the dependencies between estimates from different strata that arise since flight lines extend over several strata. An evaluation by simulated sampling in an artificial population based on data from a survey in Hedmark County, Norway, showed that the proposed estimators and their variance estimators performed well in the case of simple random sampling in both stages. In such cases, the ratio and poststratified estimators improved the precision of AGB estimates by 30% and 70%, respectively, in comparison with the earlier suggested estimator.

Key words: two-stage sampling, large-scale surveys, LULUCF reporting, REDD+.

Résumé : Pour estimer la biomasse aérienne (BA) sur de grandes superficies, les plans d'échantillonnage à deux degrés, utilisant le balayage laser aéroporté (BLA) comme outil d'échantillonnage par bandes combiné au sous-échantillonnage de parcelles de terrain, ont été appliqués avec succès dans plusieurs études. Cependant, des études ont mis en évidence des problèmes concernant l'estimateur proposé, en partie liés à la longueur inégale des lignes de vol dans les zones de forme irrégulière. Dans cet article, nous présentons pour ces plans d'échantillonnage à deux degrés un estimateur quotient assisté par un modèle qui utilise la superficie de la bande de BLA comme variable auxiliaire. L'estimateur proposé est en outre mis au point pour l'estimation dans les sous-populations et pour l'estimation poststratifiée. Pour obtenir un estimateur de variance de l'estimateur poststratifié, nous avons examiné les dépendances entre les estimations de différentes strates qui surviennent parce que les lignes de vol couvrent plusieurs strates. Une évaluation par échantillonnage simulé dans une population artificielle, basée sur les données d'une enquête dans le comté de Hedmark, en Norvège, a montré que les estimateurs proposés et leurs estimateurs de variance donnaient de bons résultats pour les deux degrés dans le cas de l'échantillonnage aléatoire simple. Dans de tels cas, les estimateurs quotient et poststratifié ont amélioré la précision des estimations de BA de respectivement 30 et 70% par rapport à l'estimateur suggéré jusqu'ici. [Traduit par la Rédaction]

Mots-clés : échantillonnage à deux degrés, enquêtes à grande échelle, rapport sur l'utilisation des terres, les changements d'affectation des terres et la foresterie (LULUCF), réduction des émissions issues de la déforestation et de la dégradation forestière (REDD+).

Introduction

Aboveground tree biomass (AGB) is the largest live biomass component of the forest carbon pool, and methods for its estimation have come in focus for LULUCF (land use, land-use change, and forestry) sector reporting, as well as for the REDD+ (reducing emissions from deforestation and forest degradation) mechanism. National Forest Inventories (NFIs) are important in this context (Maniatis and Mollicone 2010), but adaptations are needed (Cienciala et al. 2008). NFIs generally have large sample sizes, resulting in precise estimates at the national level but typically less precise estimates for smaller regions or subpopulations, e.g., certain land cover types (Köhl et al. 2011). Remote sensing data may provide a means to improve the precision of these estimates (McRoberts et al. 2010). In tropical developing countries in focus for the REDD+ mechanism, there is an urgent need to find methods that link remote sensing data with limited field surveys to make the inventories feasible (Asner et al. 2010).

Among the remote sensing data sources, airborne laser scanning (ALS) has emerged as very promising for large-area estimates of AGB (Wulder et al. 2012; Zolkos et al. 2013). In tropical forests, much focus has been on modeling the relationship between AGB and ALS data and on mapping AGB (Mascaro et al. 2011; Asner et al. 2013), and so far, less attention has been paid to estimates for larger areas and the estimation of the estimates accuracy. Inventories for LULUCF sector reporting and the REDD+ mechanism might cover very large areas such as entire counties or states and acquisition of full coverage ALS data might be unfeasible due to large costs (Beets et al. 2012). As an alternative, strategies using

Received 6 April 2016. Accepted 20 July 2016.

A.H. Ringvall and G. Ståhl. Department of Forest Resource Management, Swedish University of Agricultural Sciences, S-90183 Umeå, Sweden.
L.T. Ene, E. Næsset, and T. Gobakken. Department of Ecology and Natural Resource Management, Norwegian University of Life Sciences, P.O. Box 5003, NO-1432 Ås, Norway.
T.G. Gregoire. School of Forestry and Environmental Studies, 360 Prospect St., Yale University, New Haven, CT 06511-2189, USA.
Corresponding author: Anna H. Ringvall (email: anna.ringvall@telia.com).

Fig. 1. The left panel shows the four administrative units in Hedmark County with the ALS flight lines and locations of NFI field plots. The right panel is an illustration of the resulting two-stage design with ALS strips as PSUs and the delineation of pixels as SSUs. Figure is provided in colour online.

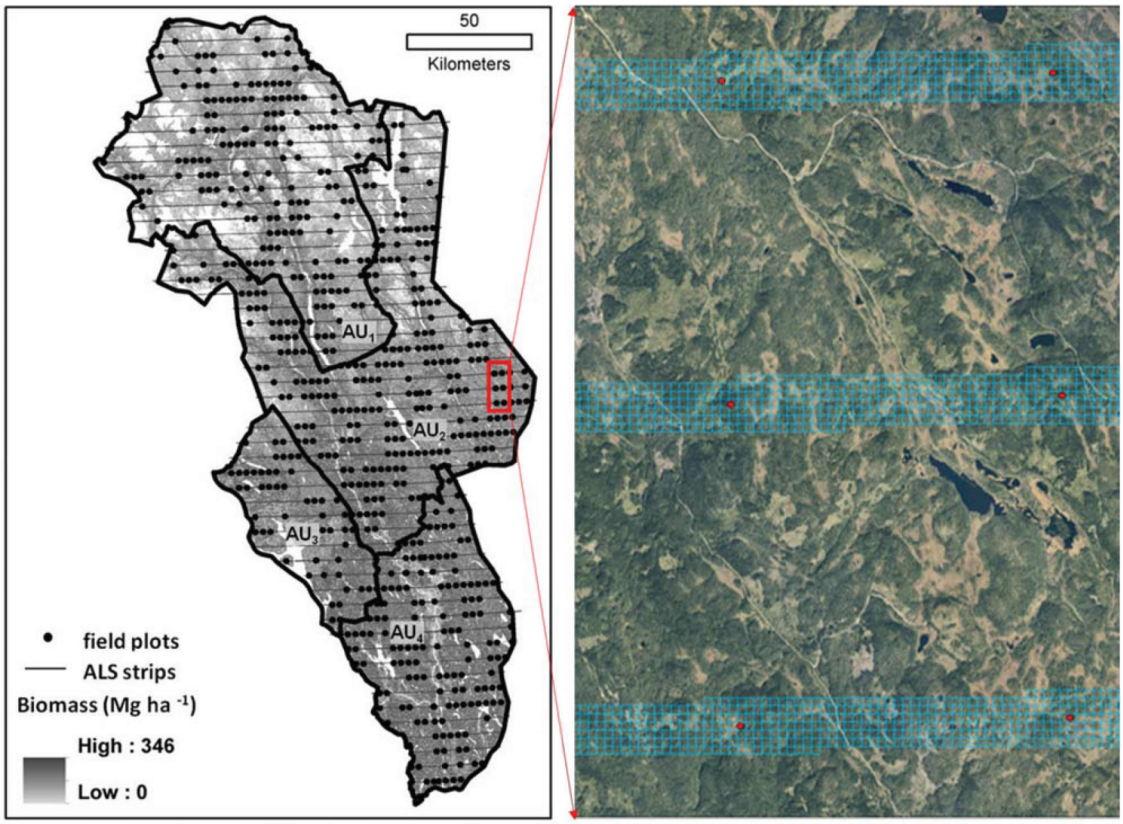

ALS data from a sampled part of the area of interest have been suggested (Parker and Evans 2004; Stephens et al. 2012). In a large-scale survey covering nearly 30 000 km² in the Hedmark County in Norway, a systematic sample of parallel ALS strips was overlaid a permanent sample of NFI field plots with measurements of AGB (Næsset et al. 2009; Fig. 1). Similar sampling designs have been used in Alaska by Andersen et al. (2009, 2011), in Finland by Saarela et al. (2015), and, recently, in Tanzania by Ene et al. (In press.). Results from a simulation study (Ene et al. 2016) indicate that sample-based ALS surveys are cost efficient in comparison with surveys with ALS that cover the whole area. Hence, strategies using ALS as a strip sampling tool are likely to be an important part of future AGB monitoring. Further, space-borne LiDAR (Nelson et al. 2009) as the proposed global ecosystem dynamics investigation (GEDI) mission (available from http://science.nasa.gov/missions/gedi/) results in designs with strip samples of LiDAR data.

Different approaches to estimation and variance estimation following sample-based ALS surveys have been tested (Ståhl et al. 2016). In Gregoire et al. (2011), a two-stage, model-assisted framework was developed and successfully applied for the Hedmark survey. Model-assisted inference is based on features of the probability sample, whereas model-based inference, as used by Ståhl et al (2011) for the same survey, is based on features of the model used to link the ALS data and the field sample (Särndal et al. 1992). Surprisingly, the estimated precision of the AGB estimates in Gregoire et al. (2011) indicated no or little improvement to the field sample alone. Later results from simulation studies in artificial populations by Ene et al. (2012, 2013) showed that the variance estimator used, based on an assumption of simple random sampling, greatly overestimated the variance with the systematic sampling design. In fact, the standard error of the model-assisted estimator was approximately 40% of the standard error of the estimator based on the field sample alone in Ene et al. (2012). The simulation studies revealed that a large portion of the variance was attributed to the large variability among ALS strips. One likely reason for the large variability is that the ALS strips have different lengths, because they extend over an irregularly shaped area (Næsset et al 2013). Ståhl et al. (2011) and Andersen et al. (2011) considered this issue by utilizing the area of the ALS strip as an auxiliary variable in ratio estimators with model-based estimates of AGB within each strip. Saarela et al. (2015) suggested selection of strips with probability proportional to size. The inferential problems encountered in these pioneering sample-based ALS inventories seem to coincide with general problems encountered in large-scale, multistage natural resource inventories (Magnussen et al. 2014).

The objective of this article is to present a model-assisted, two-stage ratio estimator utilizing the area of the ALS strip as an auxiliary variable. The motivation for developing a ratio estimator is two-fold: to improve precision of estimates and to provide a better approximation of the variance of the estimator in case of systematic sampling by taking the unequal strip length into account in the variance estimator. Further, estimates of AGB are often required not only for the entire study area, but also for certain subpopulations, e.g., for different land cover types. A ratio estimator is easily modified to an estimator of the subpopulation total by utilizing the area of the subpopulation within the ALS strip as the auxiliary variable. Wall-to-wall tessellation into land cover classes based on, e.g., satellite imagery might provide a means to improve on estimation of total AGB for the entire study area through a poststratified estimator (McRoberts et al. 2002). For complex sampling designs such as these sample-based ALS surveys, a poststratified estimator is given by the summation of the

ratio estimator for subpopulations (Smith 1991). Hence, the derived ratio estimator for a subpopulation will lead directly to a poststratified estimator of total AGB for the entire area. However, the long ALS strips extending over several strata result in dependencies between estimates from different strata that we consider when deriving a novel variance estimator for this case. The proposed estimators and variance estimators are evaluated by simulated sampling in an artificial population and compared with previously developed estimators for two-stage, model-assisted estimation.

A two-stage, model-assisted ratio estimator

Sampling design and notation

As in Gregoire et al. (2011), we will consider the combination of ALS strips and field plots with AGB measurements as a two-stage sampling design with model-assisted estimation of AGB. The area of interest is portioned into M nonoverlapping parallel strips of certain width, denoted as primary sampling units (PSUs). The strips extend over the entire survey area and, therefore, will be of unequal length (size). We denote with U_1 the population of PSUs (i.e., the M strips). In the first stage, a sample of PSUs is selected, here denoted by S_1. Each PSU is partitioned into N_i cells (pixels) with a size corresponding to the field plots. The pixels are denoted as the secondary sampling units (SSUs). In the second stage, we presume that a sample of the SSUs is selected independently within each selected PSU strip; this sample of field plots is denoted S_i. We will also, for the variance derivation, assume that the subsampling within selected PSUs is invariant of which PSUs are selected in the first stage. With the partitioning of the study area into PSUs and SSUs of certain size, the total size of the study area can be expressed in terms of the total number of pixel units $N = \sum_{i \in U_1} N_i$. Based on the field and ALS measurements, regression models are developed and used to predict AGB for all units within the selected PSUs. We focus on the estimation of either the total AGB within the study area or the total AGB for a certain subpopulation, denoted by t and t_h, respectively. These subpopulations will be denoted as strata, as they are also used for estimators based on poststratification. First, estimators, variances, and variance estimators are derived for a two-stage sampling design with arbitrary inclusion probabilities. Secondly, estimators and variance estimator are presented for the case of simple random sampling without replacement (SRSwoR) in both stages. The estimators and variance estimators of total AGB are easily modified to estimators and variance estimators of average AGB per area unit by dividing with the total area and the total area squared, respectively.

A ratio estimator of the population total

By taking the unequal PSU size into account, the total AGB within the study area is estimated by a generalized ratio estimator as (Särndal et al. 1992, p. 327)

$$\hat{t}_R = N \frac{\sum_{S_1} \hat{t}_{ir}/\pi_i}{\sum_{S_1} N_i/\pi_i} \quad (1)$$

where π_i is the inclusion probability of PSU i, and $\hat{t}_{ir}$ is the model-assisted estimator of total AGB in PSU i given as

$$\hat{t}_{ir} = \sum_{k=1}^{N_i} \hat{y}_k + \sum_{k \in S_i} \frac{y_k - \hat{y}_k}{\pi_{k|i}} \quad (2)$$

where $\hat{y}_k$ is the model-predicted AGB in pixel k in the PSU, y_k is the AGB from the field plot for pixel k, and $\pi_{k|i}$ is the inclusion probability of pixel or plot k, given that PSU i is included in the sample. This estimator is the same estimator as used in the second stage in Gregoire et al. (2011). We note that in this setup, one assisting model is being used in eq. 2 to link observed AGB data to the corresponding ALS metrics, and another model is being used in eq. 1 to adjust for varying sizes among the PSUs.

Variance and variance estimation

We derive an approximate variance of $\hat{t}_R$ by linearizing the estimator through its first-order Taylor series expansion and by conditioning on the first-stage sample (Appendix A1) whereby we obtain

$$V(\hat{t}_R) \approx \sum_{i \in U_1} \sum_{j \in U_1} C(I_i, I_j) \frac{(t_i - RN_i)}{\pi_i} \frac{(t_j - RN_j)}{\pi_j} + \sum_{i \in U_1} \frac{V(\hat{t}_{ir})}{\pi_i} \quad (3)$$

where t_i is the total AGB in PSU i and $R = \sum_{U_1} t_i / \sum_{U_1} N_i$, i.e., the AGB per pixel ratio. I_i and I_j are sample membership indicators, whose covariance is $\pi_{ij} - \pi_i \pi_j$, with π_{ij} being the joint inclusion probability of PSUs i and j. $V(\hat{t}_{ir})$ is the approximate variance of the model-assisted regression estimator of the PSU total given as $V(\hat{t}_{ir}) \approx \sum_{k=1}^{N_i} \sum_{l=1}^{N_i} C(I_k, I_l) \frac{E_k}{\pi_{k|i}} \frac{E_l}{\pi_{l|i}}$. The E terms are the deviations between a measured and predicted AGBs, i.e., $y_k - \hat{y}_k$, with $\hat{y}_k$ given by the model fitted based on the entire population rather than based on the sample as in eq. 2 (Särndal et al. 1992, p. 246).

The variance estimator is derived by estimating each component in eq. 3 by its sample counterpart (Appendix A1) and is given as

$$\hat{V}(\hat{t}_R) = \frac{N^2}{\hat{N}^2} \left(\sum_{i \in S_1} \sum_{j \in S_1} \frac{C(I_i, I_j)}{\pi_{ij}} \frac{(\hat{t}_{ir} - \hat{R}N_i)}{\pi_i} \frac{(\hat{t}_{jr} - \hat{R}N_j)}{\pi_j} + \sum_{i \in S_1} \frac{\hat{V}(\hat{t}_{ir})}{\pi_i} \right) \quad (4)$$

where $\hat{N} = \sum_{S_1} N_i/\pi_i$ and $\hat{R} = \sum_{S_1} (\hat{t}_{ir}/\pi_i) / \sum_{S_1} (N_i/\pi_i)$. The term $N^2/\hat{N}^2$ is an adjustment factor, suggested for more stable variance estimation (e.g., Thompson 1992, p. 61). Further, in ratio estimation of AGB per area unit, the variance estimator in eq. 4 is divided by N^2, and the resulting expression with $\hat{N}^2$ is the commonly used variance estimator for an estimate of a ratio (Thompson 1992, p. 61). The variance of the model-assisted estimator at the PSU level is estimated as $\hat{V}(\hat{t}_{ir}) = \sum_{k \in S_i} \sum_{l \in S_i} \frac{C(I_k I_l)}{\pi_{kl|i}} \frac{e_k}{\pi_{k|i}} \frac{e_l}{\pi_{l|i}}$ with $e_k = y_k - \hat{y}_k$, as in Gregoire et al. (2011). We note that, for example, Särndal et al. (1992, p. 238) and Mandallaz (2013) suggest to use the so called g-weighted variance estimator, where the g weights compensate for using an assisting model estimated from the sample and not an external (known) model (Mandallaz 2013). Neglecting the g weights might cause some slight underestimation of the variance (Mandallaz 2013). However, for larger sample sizes, the difference is small (Särndal et al. 1992, table 7.2).

In contrast to the variance estimator for a two-stage design with a model-assisted regression estimator presented by Särndal et al. (1992, p. 326) and used in Gregoire et al. (2011), we propose an estimator based on the model-assisted estimator of t_i (i.e., $\hat{t}_{ir}$) instead of the HT estimator $\hat{t}_i = \sum_{k \in s_i} y_k/\pi_{k|i}$, which is based solely on the second-stage field sample. Then, the variance estimator simplifies and cannot give negative variance estimates, a problem observed by the variance estimator in Gregoire et al. (2011). Given the large number of SSUs within selected PSUs, the strong relationship between predicted and true values, and the small sample size of SSUs in the second stage in this application, we also argue that $\hat{t}_{ir}$ should be much more accurate than $\hat{t}_i$. Hence, our hypothesis is that a variance estimator based on $\hat{t}_{ir}$ is more stable (i.e., has smaller variance) than a variance estimator based on $\hat{t}_i$. This has been further verified by Saarela et al. (Saarela, S., Andersen, H.-E., Grafström, A., Schnell, S., Gobakken,T., Næsset, E., Nelson, R.F.,

McRoberts R.E., Gregoire, T.G., and Ståhl, G. A new prediction-based variance estimator for two-stage model-assisted surveys of forest resources. In review.) for the two-stage model-assisted estimator by Gregoire et al (2011). Ene et al. (2012, 2013) also used the model-assisted estimates of the PSU totals in the variance estimators.

The ratio estimator with SRSwoR in both stages

In cases of SRSwoR in both stages, the ratio estimator in eq. 1 simplifies to

$$\hat{t}_R = N\frac{\sum_{i=1}^{m}\hat{t}_{ir}}{\sum_{i=1}^{m}N_i} \quad (5)$$

where m is the number of selected PSUs and

$$\hat{t}_{ir} = \sum_{k=1}^{N_i}\hat{y}_k + \frac{N_i}{n_i}\sum_{k=1}^{n_i}e_k \quad (6)$$

where n_i is the number of selected SSUs within PSU i.

The variance estimator of $\hat{t}_R$ in eq. 5 becomes

$$\hat{V}(\hat{t}_R) = \frac{N^2}{\hat{N}^2}\left[M^2\left(\frac{1}{m}-\frac{1}{M}\right)s_r^2 + \frac{M}{m}\sum_{S_1}N_i^2\left(\frac{1}{n_i}-\frac{1}{N_i}\right)s_e^2\right] \quad (7)$$

where $s_r^2 = \frac{1}{m-1}\sum_{i=1}^{m}(\hat{t}_{ir} - \hat{R}N_i)^2$ with $\hat{R} = \sum_{i=1}^{m}\hat{t}_{ir}/\sum_{i=1}^{m}N_i$ and $s_e^2 = \frac{1}{n_i-1}\sum_{k=1}^{n_i}(e_k - \bar{e}_i)^2$ with $\bar{e}_i = \sum e_k/n_i$.

The ratio estimator for poststratified estimation

Given that the total size of stratum h is known without errors, an estimator of the total AGB within the stratum is given as

$$\hat{t}_{Rh} = N_h\frac{\sum_{S_1}\hat{t}_{irh}/\pi_i}{\sum_{S_1}N_{ih}/\pi_i} \quad (8)$$

where N_h is the total number of pixels in stratum h within the entire study area, N_{ih} is the total number of pixels in stratum h in PSU i, and $\hat{t}_{irh}$ the model-assisted estimator of the total AGB in stratum h in PSU i. Further, by utilizing that the total size of stratum h in PSU i is known, the model-assisted estimator for stratum h in PSU i is given as (e.g., Särndal et al. 1992, p. 401)

$$\hat{t}_{irh} = \sum_{k=1}^{N_{ih}}\hat{y}_{kh} + \frac{N_{ih}}{\hat{N}_{ih}}\sum_{k\epsilon S_i}\frac{y_{kh}-\hat{y}_{kh}}{\pi_{k|i}} \quad (9)$$

where $\hat{y}_{kh}$ is the predicted target variable for pixel k if pixel k is in stratum h and otherwise is zero. This means that $\hat{y}_{kh}$ is the combination of the stratum-indicator variable and $\hat{y}_k$. Likewise, y_{kh} is the measured target variable in pixel k if pixel k is in stratum h and otherwise is zero. The estimated size of stratum h in PSU i is given as $\hat{N}_{ih} = \sum_{k\in S_i}1/\pi_{k|i}$. The second term of $\hat{t}_{irh}$ is a ratio estimator accounting for the random sample size in stratum h.

Finally, as suggested by Smith (1991), a poststratified estimator of the population total is given by the sum of the strata ratio estimates as

$$\hat{t}_{PS} = \sum_{h=1}^{H}\hat{t}_{Rh} = \sum_{h=1}^{H}N_h\frac{\sum_{S_1}\hat{t}_{irh}/\pi_i}{\sum_{S_1}N_{ih}/\pi_i} \quad (10)$$

where H is the total number of strata.

Variance

To derive the variance of $\hat{t}_{Rh}$, we recognize that eq. 8 is a special case of the ratio estimator $\hat{t}_R$ in eq. 1. Thus, the variance of $\hat{t}_{Rh}$ is obtained by replacing N and N_i with N_h and N_{ih}, respectively, in eq. 3. The approximate variance of $\hat{t}_{Rh}$ is then given as

$$V(\hat{t}_{Rh}) \approx \sum_{i\in U_1}\sum_{j\in U_1}C(I_i,I_j)\frac{(t_{ih}-R_hN_{ih})}{\pi_i}\frac{(t_{jh}-R_hN_{jh})}{\pi_j} + \sum_{i\in U_1}\frac{V(\hat{t}_{irh})}{\pi_i} \quad (11)$$

where t_{ih} is the PSU total for stratum h, and R_h the mean per pixel in stratum h. For PSUs without pixels in stratum h, this term will be zero. The approximate within PSU variance is derived by recognizing that the adjustment term in eq. 9 is a ratio estimator with the stratum indicator as auxiliary variable. The variance is $V(\hat{t}_{irh}) = \sum_{k=1}^{N_{ih}}\sum_{l=1}^{N_{ih}}C(I_kI_l)\frac{E_{kh}-\bar{E}_{ih}}{\pi_{k|i}}\frac{E_{lh}-\bar{E}_{ih}}{\pi_{l|i}}$ where E_{kh} is the residual $y_{kh} - \hat{y}_{kh}$ (and hence zero for units outside stratum h) and $\bar{E}_{ih} = \sum_{k=1}^{N_{ih}}E_{khl}/N_{ih}$ (cf. Särndal et al. 1992, p. 401).

In the poststratified estimator of the population total, it is important to note that there may be dependencies between estimates from different strata due to the fact that many PSUs extend over several strata, i.e., have SSUs in several different strata. This can be accounted for by first summing PSU-level estimates with the poststratified weights, e.g., as in Kim and Wang (2009). Here, we derive the variance of the poststratified estimator from the covariance matrix of the strata estimates (Appendix A2). For the derivation, we recognize that the estimator is a ratio estimator and apply the same principles as when deriving the variance of the ratio estimator (in eq. 3).

We then obtain the approximate variance of $\hat{t}_{PS}$ as

$$V(\hat{t}_{PS}) \approx \sum_{h=1}^{H}\sum_{g=1}^{H}\left(\sum_{U_1}\sum_{U_1}C(I_i,I_j)\frac{(t_{ih}-R_hN_{ih})}{\pi_i}\frac{(t_{jg}-R_gN_{jg})}{\pi_j} + \sum_{U_1}\frac{1}{\pi_i}C(\hat{t}_{irh},\hat{t}_{irg})\right) \quad (12)$$

where the term $C(\hat{t}_{irh},\hat{t}_{irg})$ is the covariance of the PSU estimators $\hat{t}_{ir}$ in stratum h and g, respectively, given as $C(\hat{t}_{irh},\hat{t}_{irg}) \approx \sum_{k=1}^{N_{ih}}\sum_{l=1}^{N_{ig}}C(I_kI_l)\frac{E_{kh}-\bar{E}_{ih}}{\pi_{k|i}}\frac{E_{lg}-\bar{E}_{ig}}{\pi_{l|i}}$.

Variance estimators can be derived following the same principles as applied to the ratio estimator (cf. eq. 4). Below, a variance estimator is given for the case of SRSwoR in both stages.

The poststratified estimator under a SRSwoR design in both stages

In case m PSUs are selected with SRSwoR in the first stage and n_i units are selected with SRSwoR in the second stage (in selected PSU i), the estimator of a stratum total in eq. 8 simplifies to

$$\hat{t}_{Rh} = N_h\frac{\sum_{i=1}^{m}\hat{t}_{irh}}{\sum_{i=1}^{m}N_{ih}} \quad (13)$$

with

$$\hat{t}_{irh} = \sum_{k=1}^{N_{ih}}\hat{y}_{kh} + \frac{N_{ih}}{n_{ih}}\sum_{k=1}^{n_{ih}}y_{kh} - \hat{y}_{kh} \quad (14)$$

where n_{ih} is the number of units selected in stratum h in PSU i in the second stage.

The variance estimator becomes

$$\hat{V}(\hat{t}_{Rh}) = \left(\frac{N_h}{\hat{N}_h}\right)^2 \left(M^2 \left(\frac{1}{m} - \frac{1}{M}\right) \frac{(m_h - 1)s^2_{rh}}{(m-1)} + \frac{M}{m} \sum_{S_1} \hat{V}(\hat{t}_{irh}) \right) \quad (15)$$

where $s^2_{rh} = \frac{1}{m_h - 1} \sum_{i=1}^{m_h} (\hat{t}_{irh} - \hat{R}_h N_{ih})^2$ with $\hat{R}_h = \sum_{S_I} \hat{t}_{irh} / \sum_{S_I} N_{ih}$.

The within PSU variance $V(\hat{t}_{irh})$ is estimated as (cf. Särndal et al. 1992, p. 393)

$$\hat{V}(\hat{t}_{irh}) = N^2_{ih} \left(\frac{1}{n_{ih}} - \frac{1}{\hat{N}_{ih}}\right) s^2_{\hat{e}_{ih}} \quad (16)$$

with $s^2_{\hat{e}_{ih}} = \frac{1}{n_{ih} - 1} \sum_{k=1}^{n_{ih}} (e_{kh} - \bar{e}_{ih})^2$, where $\bar{e}_{ih} = \frac{1}{n_{ih}} \sum_{k=1}^{n_{ih}} e_{kh}$ and $e_{kh} = y_{kh} - \hat{y}_{kh}$. In obtaining eq. 16, $n_i(n_{ih} - 1)/(n_i - 1)n_{ih}$ is approximated with 1. Särndal et al. (1992, p. 393) state that this expression is close to the conditional variance suggested by, e.g., Särndal and Hidiroglou (1989) as variance estimator for the regression estimator for a certain domain following SRSwoR (given by replacing $\hat{N}_{ih}$ in eq. 16 by N_{ih}). In applications when stratum h is covered by only a fraction of the M first stage strips the estimator in eq. 15 can be modified by the same principle (Appendix A3).

Finally, the poststratified estimator of the population total is, in case of SRSwoR, given as $\hat{t}_{PS} = \sum_{h=1}^{L} N_h (\sum_{i=1}^{m} \hat{t}_{irh} / \sum_{i=1}^{m} N_{ih})$. In the case of SRSwoR, the variance expression simplifies compared with the general case, because the covariance of the ratio estimators of the total in PSU i ($\hat{t}_{ir}$) for stratum h and g, i.e., $C(\hat{t}_{irh}, \hat{t}_{irg})$ in eq. 12 is zero for all $h \neq g$ (cf. Särndal et al. 1992, p. 266).

Consequently, the variance estimator also simplifies and is then given as

$$\hat{V}(\hat{t}_{PS}) = \sum_{h=1}^{H} \hat{V}(\hat{t}_{Rh}) + \sum_{h=1}^{H} \sum_{g \neq h} \frac{N_h}{\hat{N}_h} \frac{N_g}{\hat{N}_g} M^2 \left(\frac{1}{m} - \frac{1}{M}\right) \times \frac{\sum_{i=1}^{m} [(\hat{t}_{irh} - \hat{R}_h N_{ih}), (\hat{t}_{irg} - \hat{R}_g N_{ig})]}{m - 1} \quad (17)$$

with $\hat{V}(\hat{t}_{Rh})$ given by eq. 15.

Evaluation

The proposed estimators and variance estimators were evaluated by simulated sampling in an artificial population created based on real data from a large-scale AGB survey in Hedmark County in Norway, further described below. In the evaluation, we compared the proposed two-stage, model-assisted ratio estimator with the two-stage, model-assisted estimator proposed by Gregoire et al. (2011). These two estimators will, in the following text, be referred to as the "ratio estimator" and the "HT estimator", respectively. Both share the same model-assisted part, and the notation highlights their differences as evaluated here. The two estimators were compared for estimates of AGB per hectare for the entire study area and for estimates of AGB per hectare in four administrative units (AUs) within Hedmark County (Fig. 1). In addition, the suggested poststratified estimator was evaluated based on poststratification by the four AUs.

The empirical material and artificial population

The data collection in the Hedmark survey and the creation of the artificial population based on these data are described in detail in Ene et al. (2016) and references therein. We will give a brief description of issues of importance for the current study.

ALS data in the Hedmark survey were collected along 53 parallel flight lines that were equally spaced with a distance of 6 km (Fig. 1). The average width of ALS strips was approximately 500 m. The flight lines were located such that they covered each second row of the Norwegian NFI's sampling plots located on a 3 km × 3 km grid. In total, 662 NFI plots were covered, each plot having a size of 250 m^2. On these plots, the AGB was predicted for all trees with a diameter at breast height > 5 cm and height > 1.3 m using tree-species specific allometric models (Marklund 1988). For each plot, the tree level predictions were summed and were considered here as the true AGB of live trees on each plot. The ALS strips were partitioned into pixels of size 250 m^2.

The artificial population was created to mimic the conditions in the actual Hedmark survey. Hedmark County has an area of 27 340 km^2, a high altitudinal variation, and an increasing linear trend in the AGB per area unit from north to south (Ene et al. 2012). The artificial population was based on a delineation of forested area in the Hedmark County from land cover maps, a digital terrain model, and a satellite imagery mosaic (from Landsat 5 TM), covering the whole forest area, and resampled to pixels with area 250 m^2 to correspond to the plot size in the field survey. At first, a Gaussian copula (Nelsen 2006) was fitted to relate the AGB estimates from field plots to the ALS metrics and the spectral information from the satellite imagery mosaic in pixels covering the field plots. Then, a large sample (~100 000 observations) was generated with the copula model. Finally, observations from this sample were imputed to all pixels in the satellite imagery mosaic within the forested areas by nearest neighbor imputation. At the end, the artificial population consists of a set of images pixels (250 m^2) in forested areas, each with imputed values of ALS metrics and an imputed value of AGB (true value). The distributions of AGB on NFI plots in the Hedmark County and in the artificial population are shown in Table 1.

Simulated sampling

For the sampling simulations, the artificial population was divided into M = 625 nonoverlapping PSUs representing the ALS flight strips. These were, as in the actual Hedmark survey, oriented in an east–west direction (see Fig. 1), and the delineation followed the pixel representation in the image mosaic used as the base for creating the population. Each PSU consists of a certain number of SSUs, and each of these corresponds to one of the pixels in the artificial population. The width of each strip was 32 SSUs (pixels), except the southernmost PSU, which had a width of 29 SSUs due to the shape of the area.

In this population, repeated samples were generated by SRSwoR, with three different sampling intensities. In total, K = 100 000 samples were simulated for each design (sampling intensity). For the three designs, the number of selected PSUs in the first stage corresponded to a systematic strip spacing of 3 km, 6 km (as in the Hedmark survey), and 9 km, respectively. That resulted in m = 104, 52, and 26 selected PSUs, for each design, respectively. The size of the second-stage samples to be selected at PSU level was calculated as the average number of SSU's produced by a the systematic sampling scheme using a spacing (easting, northing) of 3 km × 3 km, 6 km × 3 km, and 9 km × 3 km, respectively. The number of selected SSUs was 2487, 1290 and 874, respectively, in each repeated sample. For each design, the sampling intensity in the second stage within selected strips were the same. Hence, the subsampling resembled the actual application in Hedmark County with the second-stage sample size being proportional to the PSU size.

Estimation

For each simulated sample, a generalized linear model was fitted based on imputed AGB values and imputed ALS metrics in the pixels (SSUs) selected in the sample (Ene et al. 2016). The generalized linear model (McCulloch and Nelder 1989) was formulated as

Table 1. Aboveground biomass distribution in field plots and in the artificial population in the four administrative units (AUs) and in total in Hedmark County, Norway.

	Field plots			Artificial population		
Administrative level	No. of plots	Mean (Mg·ha^{-1})	Standard deviation (Mg·ha^{-1})	No. of pixels (250 m^2)	Mean (Mg·ha^{-1})	Standard deviation (Mg·ha^{-1})
AU1	178	33.0	32.7	31 184 859	35.7	34.6
AU2	261	49.2	51.5	34 652 963	48.1	42.1
AU3	548	62.4	62.4	9 197 260	56.2	46.7
AU4	169	72.2	63.6	19 093 027	64.5	41.0
Total	662	51.7	53.7	94 128 109	48.1	43.6

$$\begin{cases} g(\mu) = \overline{\mathbf{X}}\boldsymbol{\beta}^{\mathrm{T}} \\ \mathrm{AGB}_i = \mu + \varepsilon_i \\ \varepsilon_i \sim \mathrm{N}(0, \sigma^2) \end{cases}$$

where the $g(\cdot)$ is the log-link function, $\overline{\mathbf{X}}\boldsymbol{\beta}^{\mathrm{T}}$ the linear predictor of the logarithm of the expected AGB value, $\overline{\mathbf{X}}$ is the model matrix, and $\boldsymbol{\beta}^{\mathrm{T}}$ is the vector of regression parameters (McCulloch and Nelder 1989, p. 26–27). The linear predictor was defined as follows:

$$\log(E[\mathrm{AGB}_i]) = \beta_0 \log(\mathrm{AGB}_i) = \beta_0 + \beta_1 \mathrm{North} + \beta_2 \log(D_{10}) + \beta_3 D_{90} + \beta_4 H_{\max} + \beta_5 \log(\mathrm{Elev}) \quad (18)$$

where North is the northing coordinates of the plot center (UTM zone 32N), D_{10} and D_{90} are canopy density metrics, $H_{\max}$ is the maximum echo height recorded on each plot, and Elev represents the ellipsoidal heights of the NFI plot centers. For details regarding the derivation of the ALS metrics from the laser acquisition in Hedmark County, see Ene et al. (2016) and Gobakken et al. (2012). When applied to the empirical data, the root mean squared error (RMSE) of the fitted model was 15.92 Mg·ha^{-1} (30.38%), and the average relative RMSE produced by 10-fold crossvalidation ($\mathrm{RMSE}_{\mathrm{CV}}$) was 33.91%.

For each simulated sample, the total AGB was estimated for the entire study area ($\hat{t}$) and for each of the four AUs ($\hat{t}_1 - \hat{t}_4$) based on the predictions of AGB for all SSUs in selected PSUs (as above) and the residuals between true and predicted AGB in SSUs selected in the second stage. With the ratio estimator, the estimates of total AGB, $\hat{t}$ and $\hat{t}_h$, were calculated with eqs. 5–6 and eqs. 13–14, respectively. For each repeated sample, we estimated the variance of the estimators $\hat{t}$ and $\hat{t}_h$. In case of the ratio estimator, $\hat{V}(\hat{t})$ was given by eq. 7 and $\hat{V}(\hat{t}_h)$ was given by eq. 15. For the poststratified estimator, $\hat{V}(\hat{t}_{\mathrm{PS}})$ was given by eq. 17. For comparison, the total AGB within the entire study areas was estimated with the (here called) HT estimator as $\hat{t} = \sum_{S_1} \hat{t}_{ir}/\pi_i$, with $\hat{t}_{ir}$ given by eq. 6 and $\pi_i = m/M$. The estimated variance, $\hat{V}(\hat{t})$, was given by eq. 7 in Ene et al. (2012). The AGB per hectare in AU h was estimated by eq. 51–51 in Gregoire et al. (2011) as its estimated variance $\hat{V}(\hat{t}_h)$ calculated by eq. 54 in Gregoire et al. (2011).

Based on the estimated totals and variances from the K simulated samples we calculated the

- observed bias as $\frac{\sum \hat{t}_k}{K} - t$, where $\hat{t}_k$ is the estimated total AGB in simulated sample number k,
- observed standard error as $\mathrm{SE} = \sqrt{\sum(\hat{t}_k - \bar{\hat{t}})^2/(K-1)}$ where $\bar{\hat{t}} = \sum \hat{t}_k/K$,
- the mean value of the estimated standard errors as $\overline{\widehat{\mathrm{SE}}} = \sum\sqrt{\hat{V}(\hat{t})_k}/K$, where $\hat{V}(\hat{t})_k$ is the estimated variance of $\hat{t}$ in simulated sample number k,
- the observed bias of the estimated standard errors as $\overline{\widehat{\mathrm{SE}}} - \mathrm{SE}$, and finally,
- the standard deviation of the estimated standard error as $\sqrt{\sum(\sqrt{\hat{V}(\hat{t})_k} - \overline{\widehat{\mathrm{SE}}})^2/(K-1)}$.

Results are presented in terms of the average AGB per hectare, calculated as $\hat{\mu} = \hat{t}/aN$ for the entire study area and $\hat{\mu}_h = \hat{t}_h/aN_h$ for AU h, where a is the area of each pixel in hectares, N is the total number of pixels in the study area, and N_h is the number of pixels in AU h. Likewise, the standard errors of the estimated AGB per hectare are obtained by dividing the standard errors of the estimated totals with the factors aN and aN_h, respectively.

Results and discussion

The observed bias of the proposed ratio and poststratified estimators and their variance estimators were in all cases small but increased slightly with decreasing sampling intensity (Table 2). The results indicate that the estimators and variance estimators perform well under a simple random sampling design. The ratio and poststratified estimators were both more precise than the earlier suggested HT estimator (Table 2). The increase in precision, in terms of standard errors, was (in comparison with the HT estimator) around 30% for the ratio estimator and around 70% for the poststratified estimator. However, the difference in precision between the HT and the ratio estimators was somewhat smaller than expected given the large differences in the size of the ALS strips in the study area. This is probably explained by the strong gradient in productivity from north to south, with a lower AGB per hectare, on average, in longer strips in the north and a higher AGB per hectare, on average, in the shorter strips in the south (Ene et al. 2012). Hence, the correlation between PSU totals of AGB and strip length is less than if the productivity had been similar across the whole study area. The geographic division in AUs partly accounts for the gradient in productivity, which also results in a large improvement in precision by poststratification based on the AUs. In this study, a rough estimate of the total AGB in the PSUs had probably been a better choice as the auxiliary variable in the ratio estimator. This estimate could for example be based on pixel-wise estimates of AGB from wall to wall satellite imagery, as used for PPS sampling in Saarela et al. (2015).

Considering the separate estimates of AGB in each of the four different AUs, the ratio estimator resulted in considerably smaller standard errors than the HT estimator (Table 3). The improvement in precision (compared with the HT estimator) was larger compared with the case of estimating AGB for the entire study area and was, in terms of standard errors, between 78% (AU4) and 88% (AU2) for the sample size of 52 PSUs. These results confirm that the internal AUs conditions are more homogenous than the entire study area, resulting in a better correlation between the size of the individual PSUs within an AU and the corresponding total AGB in each individual PSU (within the AU). The observed bias of the AGB estimates in each of the four AUs was small, like the case for the entire study area. The observed bias did not, for the sample sizes 52 and 104 PSUs, exceed 0.1% in any AU, and for

Table 2. Observed bias and observed standard error (SE) for estimates of AGB per hectare in Hedmark County with three estimators and sampling intensities (m) together with mean values of estimated standard errors and the observed bias and standard deviation of the estimated standard errors.

	Observed bias		Observed SE			Observed bias $\widehat{\overline{SE}}$		
Estimator	Mean	(%)[a]	Mean	(%)[a]	$\widehat{\overline{SE}}$	Mean	(%)[b]	Standard deviation $\widehat{\overline{SE}}$
PSU m = 104 (corresponding to strip spacing 3 km)								
HT estimator	–0.010	(–0.02)	1.590	(3.31)	1.561	–0.029	(–1.81)	0.110
Ratio estimator	0.006	(0.01)	1.142	(2.37)	1.130	–0.012	(–1.05)	0.105
Poststratified estimator	0.006	(0.01)	0.500	(1.04)	0.503	0.002	(0.46)	0.055
PSU m = 52 (corresponding to strip spacing 6 km)								
HT estimator	0.023	(0.05)	2.363	(4.91)	2.431	0.068	(2.89)	0.230
Ratio estimator	–0.002	(0.005)	1.660	(3.45)	1670	0.009	(0.56)	0.329
Poststratified estimator	0.044	(0.09)	0.749	(1.56)	0.741	–0.008	(–1.00)	0.178
PSU m = 26 (corresponding to strip spacing 9 km)								
HT estimator	0.221	(0.46)	2.807	(5.84)	2.866	0.059	(2.11)	0.350
Ratio estimator	0.049	(0.10)	2.122	(4.41)	2.057	–0.065	(–3.06)	0.630
Poststratified estimator	0.073	(0.15)	0.935	(1.94)	0.908	–0.028	(–2.97)	0.319

[a]In percent of the mean value in the population.
[b]In percent of the observed standard error of the estimated mean value.

Table 3. Observed standard error (SE) for estimates of AGB per hectare in four administrative units (AUs) with two estimators and three sampling intensities (m), together with mean values of estimated standard errors and observed bias and standard deviation of estimated standard errors.

	HT estimator				Ratio estimator			
	AU1	AU2	AU3	AU4	AU1	AU2	AU3	AU4
m = 104 PSU (corresponding to strip spacing 3 km)								
Observed SE								
Mean	4.02	5.48	9.16	8.06	0.68	1.11	1.62	1.02
(%)[a]	(11.27)	(11.39)	(16.29)	(12.50)	(1.91)	(2.31)	(2.88)	(1.59)
$\widehat{\overline{SE}}$	4.23	5.54	9.71	8.41	0.67	1.14	1.67	1.01
Bias $\widehat{\overline{SE}}$								
Mean	0.213	0.063	0.555	0.356	–0.013	0.026	0.045	–0.008
(%)[b]	(5.29)	(1.15)	(6.06)	(4.42)	(–1.85)	(2.30)	(2.76)	(–0.81)
Standard deviation $\widehat{\overline{SE}}$	0.27	0.38	1.01	0.58	0.15	0.37	1.39	0.38
m = 52 PSU (corresponding to strip spacing 6 km)								
Observed SE								
Mean	6.13	7.87	13.56	12.25	0.97	1.71	2.43	1.50
(%)[a]	(17.17)	(16.36)	(24.12)	(19.01)	(2.72)	(3.55)	(4.31)	(2.33)
$\widehat{\overline{SE}}$	6.30	7.59	14.36	12.44	1.00	1.68	2.43	1.46
Bias $\widehat{\overline{SE}}$								
Mean	0.169	–0.278	0.804	0.188	0.030	–0.028	0.000	–0.046
(%)[b]	(2.76)	(–3.54)	(5.93)	(1.54)	(3.07)	(–1.63)	(0.02)	(–3.09)
Standard deviation $\widehat{\overline{SE}}$	0.60	0.85	2.18	1.30	0.53	1.22	4.61	1.23
m = 26 PSU (corresponding to strip spacing 9 km)								
Observed SE								
Mean	7.37	9.69	15.98	14.90	1.22	2.14	3.05	1.83
(%)[a]	(20.67)	(20.15)	(28.43)	(23.12)	(3.41)	(4.44)	(5.43)	(2.85)
$\widehat{\overline{SE}}$	5.52	9.37	15.04	13.30	1.22	2.05	3.00	1.83
Bias $\widehat{\overline{SE}}$								
Mean	–1.851	–0.316	–0.936	–1.607	–0.001	–0.088	–0.054	–0.002
(%)[b]	(–25.11)	(–3.26)	(–5.86)	(–10.78)	(–0.06)	(–4.11)	(–1.77)	(–0.11)
Standard deviation $\widehat{\overline{SE}}$	0.80	1.32	3.27	1.88	0.98	2.17	8.72	2.42

[a]In percent of mean value in each subpopulation.
[b]In percent of observed standard error of estimated mean values.

the sample size 26 PSUs, it was at most 0.34% (in AU2; values not shown in tables). The observed biases of the estimated standard errors of subpopulation means were larger than the corresponding estimates for the entire study area but still modest in size and, in most cases, smaller than the observed bias of standard errors for the HT estimator (Table 3). However, the standard deviation of the estimated standard errors was in some cases larger than those of the HT estimator, especially in the smallest stratum (AU3) and with the smallest sample size. The results indicate that the proposed subpopulation estimators perform well also in the case of small sample sizes but that their variance estimators in such cases might be unstable and should be used with caution.

Designs using ALS as a strip sampling tool in combination with subsampling of field plots have now been tested in several landscapes (Gregoire et al. 2011; Andersen et al. 2011; Saarela et al.

2015; Ene et al. In press.). Simulation studies (Saarela et al. 2015; Ene et al. 2016) confirms that sample-based ALS surveys are a large improvement to field sampling alone and cost efficient in comparison with surveys based on ALS that cover the whole area. The estimators and variance estimators proposed in this study are, in theory, improvements to the earlier suggested estimators. Both the proposed ratio and poststratified estimators are reasonable estimators for all equal probability designs, estimating the AGB per area unit from the sum of predicted AGB in pixels in sampled ALS strips (corrected by the residual term) divided by the total area of sampled pixels. The derived variance estimators take both stages of sampling into account, and in case of the poststratified estimator, also the covariance between subpopulations estimates based on PSUs straddling several AUs. This is a novel feature of the variance estimator we propose. The importance of taking the covariance term, as well as the second-stage subsampling, into consideration might be more or less negligible in practice, depending on the population studied. In case the variance due to second-stage sampling is small the approximate but simpler variance estimator used by Ene et al. (In press.) might be preferable for practical reasons. The need of handling the covariance term when estimating the variance of the poststratified estimator is illustrated by calculating the added variance of the four estimates of total AGB within each strata as in "ordinary" simple random sampling. The resulting standard error of AGB per hectare for the entire study area (calculated from the observed SE of estimated AGB per hectare in Table 3 and the size of each AU in Table 1) was, for a sample size of 52 PSUs, 0.805 compared with the observed SE of the poststratified estimator, which was 0.749 (Table 2). Hence, by ignoring the covariance in this case, it leads to an overestimation of the standard error of about 6%. The overestimation indicates that, in this case, we have a negative covariance (Gregoire et al. 2016). The covariance is based on the residuals ($\hat{t}_{irh} - \hat{R}_h N_{ih}$; eq. 17) and the gradient in productivity from north to south together with the orientation of AUs (Fig. 1) results in that strips that crosses the southernmost part of an AU and the northernmost part of the next AU have, in the former AU, AGB values above that stratum average (positive residual) and, in the latter AU, AGB values below the stratum average (negative residual). However, it should be noted that both the size and sign of the covariance term depend on the features of the subpopulation studied in relation to the PSUs.

Magnussen et al. (2014) listed four general problems with model-assisted estimation in large-scale, multistage natural resource inventories: (*i*) the use of PSUs with unequal sizes, (*ii*) PSUs containing SSUs from several strata, (*iii*) a small fraction of sample units in the second (last) stage implies few sample units in small subpopulations, and (*iv*) the common use of systematic sampling designs (due to their effectiveness), and they argued that these problems favor model-based estimation. Considering two-stage ALS surveys with model-assisted estimation, we have presented solutions to the first two issues. The proposed ratio estimator also improves on estimates in subpopulations (issue *iii*), but the variance estimates were unstable with the smallest sample size. Regarding, issue *iv*, we hypothesized that the ratio estimator's SRSwoR variance estimator possibly could result in a better approximation to the variance with a systematic design than HT estimator's variance estimator. In this study, the estimated standard errors were 1.66 for the SRSwoR ratio estimator and 0.75 for the SRSwoR poststratified estimator with the sample size corresponding to strip spacing 6 km compared with the observed standard error of 0.47 in Ene et al. (2016). Hence, as an approximation to the variance in case of systematic sampling, the ratio estimator's SRSwoR variance estimator might still lead to considerable overestimation pointing to the need of alternative variance estimators, as tested with good results in Ene et al. (2013, 2016).

References

Andersen, H.-E., Barrett, T., Winterberger, K., Strunk, J., and Temesgen, H. 2009. Estimating forest biomass on the western lowlands of the Kenai Peninsula of Alaska using airborne lidar and field plot data in a model assisted sampling design [online]. *In* Proceedings of the IUFRO Division 4 Conference: Extending Forest Inventory and Monitoring Over Space and Time, Quebec City, Que., 19–22 May 2009. Available from http://blue.for.msu.edu/meeting/proceed.php [accessed 7 July 2016].

Andersen, H.-E., Strunk, J., and Temesgen, H. 2011. Using airborne light detection and ranging as a sampling tool for estimating forest biomass resources in the upper Tanana Valley of interior Alaska. West. J. Appl. For. **26**: 157–164.

Asner, G.P., Powell, G.V.N., Mascaro, J., Knapp, D.E., Clark, J.K., Jacobson, J., Kennedy-Bowdoin, T., Balaji, A., Paez-Acosta, G., Victoria, E., Secada, L., Valqui, M., and Hughes, R.F. 2010. High-resolution forest carbon stocks and emissions in the Amazon. Proc. Natl. Acad. Sci. U.S.A. **107**: 16738–16742. doi:10.1073/pnas.1004875107. PMID:20823233.

Asner, G.P., Mascaro, J., Anderson, C., Knapp, D.E., Martin, R.E., Kennedy-Bowdoin, T., van Breugel, M., Davies, S., Hall, J.S., Muller-Landau, H.C., Potvin, C., Sousa, W., Wright, J., and Bermingham, E. 2013. High-fidelity national carbon mapping for resource management and REDD+. Carbon Balance Manage. **8**: 7. doi:10.1186/1750-0680-8-7.

Beets, P.N., Brandon, A.M., Goulding, C.J., Kimberley, M.O., Paul, T.S.H., and Searles, N. 2012. The national inventory of carbon stock in New Zealand's pre-1990 planted forest using a LiDAR incomplete-transect approach. For. Ecol. Manage. **280**: 187–197. doi:10.1016/j.foreco.2012.05.035.

Cienciala, E., Tomppo, E., Snorrason, A., Broadmeadow, M., Colin, A., Dunger, K., Exnerova, Z., Lasserre, B., Petersson, H., Priwitzer, T., Sanchez, G., and Ståhl, G. 2008. Preparing emission reporting from forests: use of National Forest Inventories in European countries. Silva Fenn. **42**: 73–88.

Cochran, W.G. 1977. Sampling techniques. 3rd edition. Wiley, New York.

Ene, L.T., Næsset, E., Gobakken, T., Gregoire, T.G., Ståhl, G., Holm, S., and Nelson, R. 2012. Assessing the accuracy of regional LiDAR-based biomass estimation using a simulation approach. Remote Sens. Environ. **123**: 579–592. doi:10.1016/j.rse.2012.04.017.

Ene, L.T., Næsset, E., Gobakken, T., Gregoire, T.G., Ståhl, G., and Holm, S. 2013. A simulation approach for accuracy assessment of two-phase post-stratified estimation in large-area LiDAR biomass surveys. Remote Sens. Environ. **133**: 210–224. doi:10.1016/j.rse.2013.02.002.

Ene, L.T., Næsset, E., and Gobakken, T. 2016. Simulation-based assessment of sampling strategies for large-area biomass estimation using wall-to-wall and partial coverage airborne laser scanning surveys. Remote Sens. Environ. **176**: 328–340. doi:10.1016/j.rse.2016.01.025.

Ene, L.T., Næsset, E., Gobakken, T., Mauya, E.M., Bollandsås, O.M., Gregoire, T.G., Ståhl, G., and Zahabu, E. In press. Large-scale estimation of aboveground biomass in miombo woodlands using airborne laser scanning and national forest inventory data. Rem. Sen. Environ.

Gobakken, T., Næsset, E., Nelson, R., Bollandsås, O.M., Gregoire, T.G., Ståhl, G., Holm, S., Ørka, H.O., and Astrup, R. 2012. Estimating biomass in Hedmark County, Norway using national forest inventory field plots and airborne laser scanning. Remote Sens. Environ. **123**: 443–456. doi:10.1016/j.rse.2012.01.025.

Gregoire, T.G., Ståhl, G., Næsset, E., Gobakken, T., Nelson, R., and Holm, S. 2011. Model-assisted estimation of biomass in a LiDAR sample survey in Hedmark county, Norway. Can. J. For. Res. **41**(1): 83–95. doi:10.1139/X10-195.

Gregoire, T.G., Ringvall, A.H., Ståhl, G., and Næsset, E. 2016. Conditioning poststratified inference following two-stage, equal-probability sampling. Environ. Ecol. Stat. **23**(1): 141–154. doi:10.1007/s10651-015-0332-9.

Kim, K., and Wang, S. 2009. Second-order variance estimation in poststratified two-stage sampling. J. Stat. Plan. Infer. **139**: 2502–2510. doi:10.1016/j.jspi.2008.11.004.

Köhl, M., Lister, A., Scott, C.T., Baldauf, T., and Plugge, D. 2011. Implications of sampling design and sample size for national carbon accounting systems. Carbon Balance Manage. **6**: 10. doi:10.1186/1750-0680-6-10.

Magnussen, S., Næsset, E., and Gobakken, T. 2014. An estimator of variance for two-stage ratio regression estimators. Forest Sci. **60**: 663–676. doi:10.5849/forsci.12-163.

Mandallaz, D. 2013. Design-based properties of some small-area estimators in forest inventory with two-phase sampling. Can. J. For. Res. **43**(5): 441–449. doi:10.1139/cjfr-2012-0381.

Maniatis, D., and Mollicone, D. 2010. Options for sampling and stratification for national forest inventories to implement REDD+ under the UNFCCC. Carbon Balance Manage. **5**: 9. doi:10.1186/1750-0680-5-9.

Marklund, L.G. 1988. Biomass functions for pine, spruce and birch in Sweden. Report. Swedish University of Agricultural Sciences, Department of Forest Survey, Umeå. [In Swedish.]

Mascaro, J., Detto, M., Asner, G.P., and Muller-Landau, H.C. 2011. Evaluating uncertainty in mapping forest carbon with airborne LiDAR. Remote Sens. Environ. **115**: 3770–3774. doi:10.1016/j.rse.2011.07.019.

McCulloch, C.E., and Nelder, J.A. 1989. Generalized linear models. 2nd ed. Chapman and Hall, London, UK.

McRoberts, R.E., Wendt, D.G., Nelson, M.D., and Hansen, M.H. 2002. Using a land cover classification based on satellite imagery to improve the precision of forest inventory area estimates. Remote Sens. Environ. **81**: 36–44. doi:10.1016/S0034-4257(01)00330-3.

McRoberts, R.E., Tomppo, E.O., and Næsset, E. 2010. Advances and emerging issues in national forest inventories. Scand. J. Forest. Res. **25**: 368–381. doi:10.1080/02827581.2010.496739.

Næsset, E., Gobakken, T., and Nelson, R. 2009. Sampling and mapping forest volume and biomass using airborne LIDARs. *In* Proceedings of the Eighth Annual Forest Inventory and Analysis Symposium, Monterey, Calif., 16–19 October 2006. United States Department of Agriculture, Forest Service, Washington, D.C. General Technical Report, WO-79. pp. 297–301.

Næsset, E., Gobakken, T., Bollandsås, O.M., Gregoire, T.G., Nelson, R., and Ståhl, G. 2013. Comparison of precision of biomass estimates in regional field sample surveys and airborne LiDAR-assisted surveys in Hedmark County, Norway. Remote Sens. Environ. **130**: 108–120. doi:10.1016/j.rse.2012.11.010.

Nelsen, R.B. 2006. An introduction to copulas. 2nd edition. Springer, New York. doi:10.1007/0-387-28678-0.

Nelson, R., Boudreau, J., Gregoire, T.G., Margolis, H., Næsset, E., Gobakken, T., and Ståhl, G. 2009. Estimating Quebec provincial forest resources using ICESat/GLAS. Can. J. For. Res. **39**(4): 862–881. doi:10.1139/X09-002.

Parker, R.C., and Evans, D.L. 2004. An application of LiDAR in a double-sampling forest inventory. West. J. Appl. For. **19**: 95–101.

Saarela, S., Grafström, A., Ståhl, G., Kangas, A., Holopainen, M., Tuominen, S., Nordkvist, K., and Hyyppä, J. 2015. Model-assisted estimation of growing stock volume using different combinations of LiDAR and Landsat data as auxiliary information. Remote Sens. Environ. **158**: 431–440. doi:10.1016/j.rse.2014.11.020.

Särndal, C.-E., and Hidiroglou, M.A. 1989. Small domain estimation: a conditional analysis. JASA, **84**: 266–275.

Särndal, C.-E., Swensson, B., and Wretman, J. 1992. Model assisted survey sampling. Springer-Verlag, New York.

Smith, T.M.F. 1991. Post-stratification. Statistician, **40**: 315–323. doi:10.2307/2348284.

Ståhl, G., Holm, S., Gregoire, T.G., Gobakken, T., Næsset, E., and Nelson, R. 2011. Model-based inference for biomass estimation in a LiDAR sample survey in Hedmark County, Norway. Can. J. For. Res. **41**(1): 96–107. doi:10.1139/X10-161.

Ståhl, G., Saarela, S., Schnell, S., Holm, S., Breidenbach, J., Healey, S.P., Patterson, P.L., Magnussen, S., Næsset, E., McRoberts, R.E., and Gregoire, T.G. 2016. Use of models in large-area forest surveys: comparing model-assisted, model-based and hybrid estimation. Forest Ecosystems, **3**: 5. doi:10.1186/s40663-016-0064-9.

Stephens, P.R., Kimberley, M.O., Beets, P.N., Paul, T.S.H., Searles, N., Bell, A., Brack, C., and Broadley, J. 2012. Airborne scanning LiDAR in a double sampling forest carbon inventory. Remote Sens. Environ. **117**: 348–357. doi:10.1016/j.rse.2011.10.009.

Thompson, S.K. 1992. Sampling. Wiley, New York. doi:10.1002/9781118162934.

Wulder, M.A., White, J.C., Nelson, R.F., Næsset, E., Ørka, H.O., Coops, N.C., Hilker, T., Bater, C.W., and Gobakken, T. 2012. Lidar sampling for large-area forest characterization: a review. Remote Sens. Environ. **121**: 196–209. doi:10.1016/j.rse.2012.02.001.

Zolkos, S.G., Goetz, S.J., and Dubayah, R. 2013. A meta-analysis of terrestrial aboveground biomass estimation using lidar remote sensing. Remote Sens. Environ. **128**: 289–298. doi:10.1016/j.rse.2012.10.017.

Appendix A

A1. Variance of the ratio estimator

To derive the variance of $\hat{t}_R$, we approximate the variance with its first-order Taylor series expansion whereby we obtain

$$V(\hat{t}_R) = N^2 V(\hat{R}) \approx \frac{N^2}{(E(\hat{N}))^2} V\left(\sum_{S_1} \frac{\hat{t}_{ir}}{\pi_i} - R\sum_{S_1}\frac{N_i}{\pi_i}\right) \quad \text{(A1)}$$

The $V(\cdot)$ part on the right-hand side is then expanded to

$$V(\cdot) = V\left(\sum_{S_1}\frac{\hat{t}_{ir}}{\pi_i}\right) + R^2 V\left(\sum_{S_1}\frac{N_i}{\pi_i}\right) - 2RC\left(\sum_{S_1}\frac{\hat{t}_{ir}}{\pi_i}, \sum_{S_1}\frac{N_i}{\pi_i}\right) \quad \text{(A2)}$$

To further develop the three terms in eq. A2, we condition on the first-stage sample and utilize that $V(\cdot) = V_I E_{II}(\cdot|S_1) + E_I V_{II}(\cdot|S_1)$ and $C(\cdot,\cdot) = C_I E_{II}(\cdot,\cdot|S_1) + E_I C_{II}(\cdot,\cdot|S_1)$, where the subscripts denotes the stages. With this approach, the first term on the right-hand side will be

$$V\left(\sum_{S_1}\frac{\hat{t}_{ir}}{\pi_i}\right) = V_I\left(\sum_{S_1}\frac{t_i}{\pi_i}\right) + E_I V_{II} = \sum_{i\in U_1}\sum_{j\in U_1} C(I_i, I_j)\frac{t_i}{\pi_i}\frac{t_j}{\pi_j} + E_I V_{II} \quad \text{(A3)}$$

where I_i and I_j are sample membership indicators, whose covariance is $\pi_{ij} - \pi_i\pi_j$. The $E_I V_{II}$ term will, due to the independent selection of the second-stage sample within each selected PSU, be

$$E_I V_{II}\left(\sum_{S_1}\frac{\hat{t}_{ir}}{\pi_i}\right) = E_I\left(\sum_{S_1}\frac{V(\hat{t}_{ir})}{\pi_i^2}\right) = \sum_{U_1}\frac{V(\hat{t}_{ir})}{\pi_i} \quad \text{(A4)}$$

where $V(\hat{t}_{ir})$ is the variance of the estimator of the PSU total.

To address the second term of eq. A2, there is no need to apply a conditioning approach, and the variance part of the term can be obtained directly as

$$V\left(\sum_{S_1}\frac{N_i}{\pi_i}\right) = \sum_{U_1}\sum_{U_1} C(I_i, I_j)\frac{N_i}{\pi_i}\frac{N_j}{\pi_j} \quad \text{(A5)}$$

Regarding the covariance in the third term of eq. A2, conditioning on the first-stage sample leads to

$$C_{II}\left(\sum_{S_1}\frac{\hat{t}_{ir}}{\pi_i}, \sum_{S_1}\frac{N_i}{\pi_i}\right) = 0 \quad \text{(A6)}$$

and thus $E_I C_{II} = 0$, because the only random terms involved are related to the estimation of the PSU totals (there is no random component linked to the PSU sizes when we condition on the first-stage sample). However, studying the component $C_I E_{II}$, we obtain the following:

$$C_I\left(\sum_{S_1}\frac{\hat{t}_{ir}}{\pi_i}, \sum_{S_1}\frac{N_i}{\pi_i}\right) = \sum_{i\in U_1}\sum_{j\in U_2} C(I_i, I_j)\frac{t_i}{\pi_i}\frac{N_j}{\pi_j} \quad \text{(A7)}$$

By putting all components together, the variance of $\hat{t}_R$ is given as

$$V(\hat{t}_R) \approx \sum_{i\in U_I}\sum_{j\in U_I} C(I_i, I_j)\frac{t_i}{\pi_i}\frac{t_j}{\pi_j} + \sum_{i\in U_I}\frac{V(\hat{t}_{ir})}{\pi_i} + R^2\sum_{i\in U_I}\sum_{j\in U_I} C(I_i, I_j)\frac{N_i}{\pi_i}\frac{N_j}{\pi_j} - 2R\sum_{i\in U_I}\sum_{j\in U_I} C(I_i, I_j)\frac{t_i}{\pi_i}\frac{N_j}{\pi_j} \quad \text{(A8)}$$

For the variance estimator, we propose to estimate the first term in eq. A8 with

$$\sum_{i\in S_1}\sum_{j\in S_1}\frac{C(I_i, I_j)}{\pi_{ij}}\frac{\hat{t}_{ir}}{\pi_i}\frac{\hat{t}_{jr}}{\pi_j} - \sum_{i\in S_1}\frac{\hat{V}(\hat{t}_{ir})}{\pi_i}\left(\frac{1}{\pi_i} - 1\right) \quad \text{(A9)}$$

The correction form is the 'standard' deduction made to compensate for the overestimation due to using estimated rather than measured PSU totals (e.g., Särndal et al. 1992, p. 137). However, we propose an estimator based on the model-assisted estimator of t_i (i.e., $\hat{t}_{ir}$) instead of the HT estimator $\hat{t}_i = \sum_{k\in s_i} y_k/\pi_{k|i}$, based solely on the second-stage field sample as suggested by Särndal et al. (1992, p. 326). The second term in eq. A8 is estimated with $\sum_{i\in S_I}\hat{V}(\hat{t}_{ir})/\pi_i^2$ (as usual), and the first two terms are then simultaneously estimated by

$$\sum_{i\in S_1}\sum_{j\in S_1}\frac{C(I_i, I_j)}{\pi_{ij}}\frac{\hat{t}_{ir}}{\pi_i}\frac{\hat{t}_{jr}}{\pi_j} + \sum_{i\in S_1}\frac{\hat{V}(\hat{t}_{ir})}{\pi_i} \quad \text{(A10)}$$

The two remaining terms are estimated by their sample counterparts, and the variance estimator becomes

$$\text{(A11)}\quad \hat{V}(\hat{t}_R) = \sum_{i\in S_1}\sum_{j\in S_1}\frac{C(I_i, I_j)}{\pi_{ij}}\frac{\hat{t}_{ir}}{\pi_i}\frac{\hat{t}_{jr}}{\pi_j} + \sum_{i\in S_1}\frac{\hat{V}(\hat{t}_{ir})}{\pi_i} + \hat{R}^2\sum_{i\in S_1}\sum_{j\in S_1}\frac{C(I_i, I_j)}{\pi_{ij}}\frac{N_i}{\pi_i}\frac{N_j}{\pi_j} - 2\hat{R}\sum_{i\in S_1}\sum_{j\in S_1}\frac{C(I_i, I_j)}{\pi_{ij}}\frac{\hat{t}_{ir}}{\pi_i}\frac{N_j}{\pi_j}$$

given that the sampling design is such that $\pi_{ij} > 0$ for all pairs i and j.

A2. Variance of the poststratified estimator

Following Ståhl et al. (2011), we derive the variance of the poststratified estimator of the population total, $\hat{t}_{PS}$, from the generic formula

$$\text{(A12)}\quad V(\hat{t}_{PS}) = \sum_{h=1}^{H}\sum_{g=1}^{H}C(\hat{t}_{Rh}, \hat{t}_{Rg}) = \sum_{h=1}^{H}\sum_{g=1}^{H}N_hN_gC(\hat{R}_{Rh}, \hat{R}_{Rg})$$

By applying the customary Taylor linearization for ratio estimators (as above)

$$\text{(A13)}\quad C(\hat{t}_{Rh}, \hat{t}_{Rg}) \approx \frac{N_hN_g}{E(\hat{N}_h)E(\hat{N}_g)}C\left(\sum_{S_I}\frac{\hat{t}_{irh}}{\pi_i} - R_h\sum_{S_I}\frac{N_{ih}}{\pi_i}, \sum_{S_I}\frac{\hat{t}_{irg}}{\pi_i} - R_{kg}\sum_{S_I}\frac{N_{ig}}{\pi_i}\right)$$

the $C(\cdot)$ expression is then further expanded to (cf. Cochran 1977 p. 181)

$$\text{(A14)}\quad C(\cdot) = C\left(\sum_{S_I}\frac{\hat{t}_{irh}}{\pi_i}, \sum_{S_I}\frac{\hat{t}_{irg}}{\pi_i}\right) + R_hR_gC\left(\sum_{S_I}\frac{N_{ih}}{\pi_i}, \sum_{S_I}\frac{N_{ig}}{\pi_i}\right) - R_hC\left(\sum_{S_I}\frac{\hat{t}_{irg}}{\pi_i}, \sum_{S_I}\frac{N_{ih}}{\pi_i}\right) - R_gC\left(\sum_{S_I}\frac{\hat{t}_{irh}}{\pi_i}, \sum_{S_I}\frac{N_{ig}}{\pi_i}\right)$$

As for the derivation of the variance of the ratio estimator, each of these terms is further developed by conditioning on the outcome of the first-stage sample and utilizing that $C(\cdot,\cdot) = C_IE_{II}(\cdot,\cdot|S_1) + E_IC_{II}(\cdot,\cdot|S_1)$. With this approach, the first component of the first term of eq. A11 will be

$$\text{(A15)}\quad C_IE_{II}\left(\sum_{S_I}\frac{\hat{t}_{irh}}{\pi_i}, \sum_{S_I}\frac{\hat{t}_{irg}}{\pi_i}\middle|S_I\right) = C\left(\sum_{S_I}\frac{t_{ih}}{\pi_i}, \sum_{S_I}\frac{t_{ig}}{\pi_i}\right) = \sum_{U_I}\sum_{U_I}C(I_i, I_j)\frac{t_{ih}}{\pi_i}\frac{t_{jg}}{\pi_j}$$

and the second component will be

$$\text{(A16)}\quad E_IC_{II}\left(\sum_{S_I}\frac{\hat{t}_{irh}}{\pi_i}, \sum_{S_I}\frac{\hat{t}_{irg}}{\pi_i}\middle|S_I\right) = E_I\left(\sum_{S_I}\frac{1}{\pi_i^2}C(\hat{t}_{irh}, \hat{t}_{irg})\right) = \sum_{U_I}\frac{1}{\pi_i}C(\hat{t}_{irh}, \hat{t}_{irg})$$

due to the assumption of an independent selection of the second-stage sample within each selected PSU. The term $C(\hat{t}_{irh}, \hat{t}_{irg})$ is the covariance of the PSU estimators $\hat{t}_{ir}$ in stratum h and g, respectively. As earlier, to address the second term of eq. A11, there is no need to apply a conditioning approach because no subsampling is involved. In the third (and fourth) terms of eq. A14, $C_{II}\left(\sum_{S_I}\frac{\hat{t}_{irg}}{\pi_i}, \sum_{S_I}\frac{N_{ih}}{\pi_i}|S_1\right) = 0$ and $E_IC_{II} = 0$ but $C_IE_{II} = C_I\left(\sum_{S_I}\frac{t_{ig}}{\pi_i}, \sum_{S_I}\frac{N_{ih}}{\pi_i}\right) = \sum_{U_I}\sum_{U_I}C(I_i, I_j)\frac{t_{ig}}{\pi_i}\frac{N_{jh}}{\pi_j}$.

By putting all components together, we obtain

$$\text{(A17)}\quad V(\hat{t}_{PS}) \approx \sum_{h=1}^{H}\sum_{g=1}^{H}\left(\sum_{U_I}\sum_{U_I}C(I_i, I_j)\frac{t_{ih}}{\pi_i}\frac{t_{jg}}{\pi_j} + \sum_{U_I}\frac{1}{\pi_i}C(\hat{t}_{irh}, \hat{t}_{irg}) + R_hR_g\sum_{U_I}\sum_{U_I}C(I_i, I_j)\frac{N_{ih}}{\pi_i}\frac{N_{jg}}{\pi_j} + R_h\sum_{U_I}\sum_{U_I}C(I_i, I_j)\frac{t_{ig}}{\pi_i}\frac{N_{jh}}{\pi_j} + R_g\sum_{U_I}\sum_{U_I}C(I_i, I_j)\frac{t_{ih}}{\pi_i}\frac{N_{jg}}{\pi_j}\right)$$

A3. The variance estimator of the stratum estimator in case of SRSwoR

In case m PSUs are selected from M available PSUs with SRSwoR, an estimator of the variance of $\hat{t}_{Rh}$ is given as

$$\text{(A18)}\quad \hat{V}(\hat{t}_{Rh}) = \left(\frac{N_h}{\hat{N}_h}\right)^2\left(M^2\left(\frac{1}{m} - \frac{1}{M}\right)\frac{(m_h - 1)s_{rh}^2}{(m - 1)} + \frac{M}{m}\sum_{S_1}\hat{V}(\hat{t}_{irh})\right)$$

where $s_{rh}^2 = \frac{1}{m_h - 1}\sum_{i=1}^{m_h}(\hat{t}_{irh} - \hat{R}_hN_{ih})^2$ and m_h is the number of selected PSUs in S_1 with any SSU in stratum h. The first part of eq. 1, i.e., the between PSU variance, can be further elaborated as

$$\frac{(M_h\bar{N}_h)^2}{\left(\frac{M}{m}m_h\widehat{\bar{N}}_h\right)^2}M^2\left(\frac{1}{m} - \frac{1}{M}\right)\frac{(m_h - 1)s_r^2}{(m - 1)} = \left(\frac{\bar{N}_h}{\widehat{\bar{N}}_h}\right)^2M_h^2\left(\frac{m}{m_h}\right)^2\left(\frac{1}{M} - \frac{1}{m}\right) \times \frac{(m_h - 1)s_r^2}{(m - 1)} = \left(\frac{\bar{N}_h}{\widehat{\bar{N}}_h}\right)^2M_h^2\left(\frac{1}{m_h} - \frac{1}{\hat{M}_h}\right)\frac{m}{m_h}\frac{(m_h - 1)s_r^2}{(m - 1)}$$

where M_h is the total number of PSU in U_1 that have any SSU within stratum h, $\bar{N}_h = N_h/M_h$, $\bar{N}_h = \hat{N}_h/\hat{M}_h$, and $\hat{M}_h = \frac{M}{m}m_h$. Following Särndal et al. (1992, p. 404), we approximate $\frac{m}{m-1}\frac{m_h - 1}{m_h}$ with 1. In combination with the second part of eq. A18 (the within PSU variance), the variance estimator becomes

$$\text{(A19)}\quad \hat{V}(\hat{t}_{Rh}) = \left(\frac{\bar{N}_h}{\widehat{\bar{N}}_h}\right)^2\left(M_h^2\left(\frac{1}{m_h} - \frac{1}{\hat{M}_h}\right)s_{rh}^2 + \left(\frac{M_h}{m_h}\right)^2\frac{m}{M}\sum_{S_1}\hat{V}(\hat{t}_{irh})\right)$$

because $\left(\frac{N_h}{\hat{N}_h}\right)^2\frac{M}{m} = \left(\frac{\bar{N}_h}{\widehat{\bar{N}}_h}\right)^2\left(\frac{M_h}{m_h}\right)^2\frac{m}{M}$.